Sensors and Materials, Vol. 38, No. 5 (2026) 2583–2596
MYU Tokyo

S & M 4455

Maximum Power Point Tracker for Photovoltaic Module Arrays with Automatic Step Size Adjustment

Kuei-Hsiang Chao,* Cheng-Ze Li, and Kuan-Ting Lee

Department of Electrical Engineering, National Chin-Yi University of Technology
No. 57, Sec. 2, Zhongshan Rd., Taiping Dist., Taichung 41170, Taiwan

(Received July 7, 2025; accepted March 25, 2026)

Keywords: photovoltaic module array, maximum power point tracking, improved incremental conductance method, sensors, *P–V* characteristic curve, dynamic response, steady-state performance

In this paper, we propose an improved incremental conductance (IINC) method with automatic step size adjustment for maximum power point tracking (MPPT) in photovoltaic module arrays (PVMAs). The proposed method achieves MPPT by utilizing simple voltage and current sensors to feedback the output voltage and current of the PVMAs. Owing to changes in solar irradiance and temperature, the maximum power output of the PVMA varies. When the traditional incremental conductance (INC) is used for MPPT, if the tracking step size is very small and fixed, it results in excessively long tracking times. Conversely, if a large and fixed tracking step size is used, the tracking speed may increase; however, this can lead to unstable operation near the maximum power point (MPP), causing large oscillations around the point. As a result, the overall output power of the PVMA is reduced. To address this issue, we propose in this paper an IINC, aimed at enhancing the output power of the PVMA. First, the initial voltage for MPPT was set to 0.8 times the MPP voltage V_{mp} of the PVMA under standard test conditions. At the same time, the tracking step size was automatically adjusted on the basis of the slope of the power–voltage (*P–V*) characteristic curve of the PVMA. Finally, experimental tests were conducted under various solar irradiance conditions using both the conventional INC and IINC for the MPPT of the PVMA. The results demonstrate that the proposed IINC offers superior dynamic response and steady-state performance compared with the traditional INC.

1. Introduction

A photovoltaic power generation system consists of a photovoltaic module array (PVMA), a power conditioner,[1,2] and a power distribution system. The power conditioner, which also incorporates maximum power point tracking (MPPT) functionality, includes components such as DC/AC inverters, DC/DC converters, a system controller, and protection devices. These components work together to ensure the smooth operation of the photovoltaic power generation system.

*Corresponding author: e-mail: chaokh@ncut.edu.tw
https://doi.org/10.18494/SAM5840

ISSN 0914-4935

Connecting the PVMA directly to the load may cause its output power to be affected by the load, making it difficult to achieve maximum power efficiency. To address this issue, an MPPT controller[1] is used to enable the PVMA to operate at the optimal power output point under varying solar irradiance, ensuring that the system achieves maximum generation efficiency under different operating conditions. Therefore, the MPPT controller plays a crucial role in improving the overall performance of photovoltaic power generation systems, making them reliable and efficient renewable energy sources. Moreover, the PVMA generates different power–voltage (P–V) characteristic curves[3] under varying ambient temperature and solar irradiance, and the maximum power point (MPP) also shifts. Therefore, it is necessary to track the MPP.

Current commercial power controllers commonly use traditional MPPT techniques, including the perturbation and observation (P&O) method,[4,5] constant voltage method (CVM),[6] power feedback method (PFM),[7] and incremental conductance (INC) method.[8,9]

The P&O method observes changes in output power through voltage perturbations to adjust the tracking direction.[5] This method is advantageous owing to its simple structure and minimal parameter requirements. However, it is prone to oscillations near the MPP, which can lead to power loss. Additionally, the choice of perturbation step size significantly affects the tracking performance. A small step size can inhibit oscillations but can also reduce the tracking speed. Conversely, a large step size increases the tracking speed but can cause significant oscillations near the MPP. Moreover, under rapidly changing environmental conditions, the tracking direction may not adjust quickly enough, leading to erroneous judgments. Thus, further improvement is needed to ensure the stable and accurate tracking of the MPP.

The CVM uses the MPP voltage of the PVMA, measured under high solar irradiance conditions, as a reference value.[6] The output voltage of the array is adjusted to match this reference value, thereby tracking the MPP. While this method is simple, easy to implement, and not prone to oscillations, its tracking accuracy decreases significantly when environmental conditions change rapidly. Consequently, it may fail to track the new MPP in time.

Furthermore, the PFM uses voltage and current sensors to feedback the voltage and current of the PVMA,[7] thereby calculating the current output power. By analyzing the output power and the rate of change in output voltage (dP/dV), this method determines the location of the MPP and the direction for the next tracking step. This method is simple to implement, reduces power loss, and improves overall efficiency. However, owing to the fixed tracking step size, it exhibits poor speed response and steady-state performance. Moreover, the likelihood of the system operating at a point where the power–voltage curve slope is zero is extremely low. The relatively complex control algorithm also makes it difficult to achieve high-precision control.

The INC method, on the other hand, tracks the MPP by adjusting the output conductance of the PVMA.[8] It is simple in structure, requires no complex calculations, and uses the comparison between dynamic and static conductances ($dI/dV = -I/V$) for logical decision-making. Here, V and I represent the output voltage and current, whereas dI/dV and I/V are the dynamic and static conductances, respectively. This method improves both the tracking accuracy and dynamic response of the P&O method, especially under rapidly changing environmental conditions.

Given the advantages and disadvantages of the traditional MPPT methods described above, in this study, we selected the INC method for the MPPT of the PVMA, as it provides higher dynamic response performance and tracking capability than the P&O method, along with superior reliability. Therefore, on the basis of the traditional INC method, we propose an improved incremental conductance (IINC) method, which uses a fixed initial tracking voltage. By adjusting the tracking step size according to the slope of the *P–V* characteristic curve in different operating regions, this method enhances the tracking of the MPP and improves the overall energy generation efficiency of the PVMA.

2. MPPT Architecture of PVMAs

We used Kyocera KS20 photovoltaic modules, manufactured by Kyocera Corporation of Japan (as specified in Table 1),[10] to form a four-series, three-parallel PVMA. The simulation results of the current–voltage (*I–V*) and *P–V* characteristic curves for the four-series, three-

Table 1
Specifications of Kyocera KS20 photovoltaic module.

Maximum power (Pmp)	20 W
Open-circuit voltage (Voc)	21.5 V
Short-circuit current (Isc)	1.24 A
Voltage at MPP (Vmp)	16.9 V
Current at MPP (Imp)	1.2 A

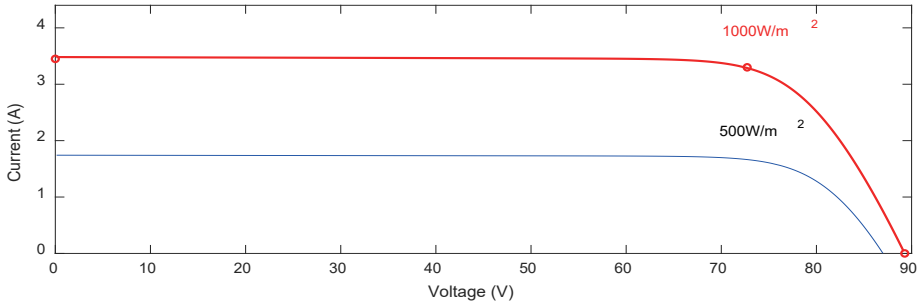

Fig. 1. (Color online) *I–V* characteristic curve of four-series, three-parallel PVMA at 25 °C under different solar irradiance intensities.

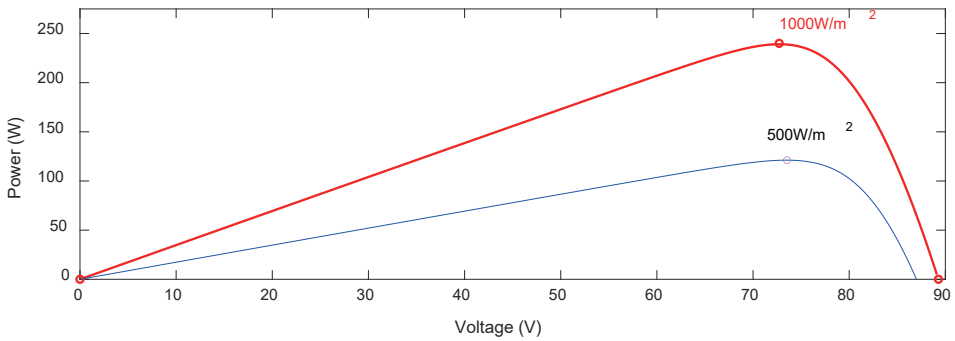

Fig. 2. (Color online) characteristic curve of four-series, three-parallel PVMA at 25 °C under different solar irradiance intensities.

Table 2
Output values of four-series, three-parallel PVMA at 25°C under different solar irradiance intensities.

Parameter value	Solar irradiance	
	1000 W/m^2	500 W/m^2
Short-circuit current (I_{sc})	4.031 A	2.241 A
Power at MPP (P_{mp})	245.9 W	122.9 W
Current at MPP (I_{mp})	3.671 A	2.040 A
Voltage at MPP (V_{mp})	67.0 V	60.3 V

parallel array formed by the Kyocera KS20 photovoltaic modules, under solar irradiance intensities of 1000 and 500 W/m², are shown in Figs. 1 and 2, respectively. Table 2 presents the short-circuit current, MPP voltage, MPP current, and maximum output power values for the four-series, three-parallel PVMA under solar irradiance intensities of 1000 and 500 W/m², with a temperature of 25 °C.

Figure 3 illustrates the MPPT architecture of the proposed IINC method. This system consists of two subsystems: (1) a boost converter and (2) the MPPT controller based on the IINC method. The controller uses a differential amplifier to feedback the voltage and current of the PVMA, and a TMS320F2809 digital signal processor (DSP)[11] is employed to implement the IINC algorithm. The DSP controls the switching on and off times of the boost converter to track the MPP of the PVMA.

3. Design of Boost Converter

Figure 4 shows the main circuit diagram of the boost converter, where the circuit consists of a switch, fast diode, energy storage inductor, and filtering capacitor. The switch is controlled by pulse width modulation (PWM) to regulate its on and off states.[12]

We can observe that the inductor satisfies the volt-second balance; thus, the output voltage (V_o) can be derived as

$$V_O = \frac{V_S}{(1-D)T}. \tag{1}$$

Since $0 \le D \le 1$, it follows that $V_s \le V_o \le \infty$. Therefore, the output voltage of the converter (V_o) is always greater than or equal to the input voltage (V_s), which is why this converter is referred to as a boost converter. When the boost converter operates at a higher switching frequency, the sizes of the energy storage inductor and the filtering capacitor can be reduced. Thus, we selected 25 kHz as the switching frequency for the boost converter. After the design, the component specifications of the boost converter are listed in Table 3.[13]

4. Traditional INC Method

The INC method calculates the current power on the basis of the feedback from the voltage and current. Then, the change rate of output power and output voltage (dP/dV) from Eq. (2) is

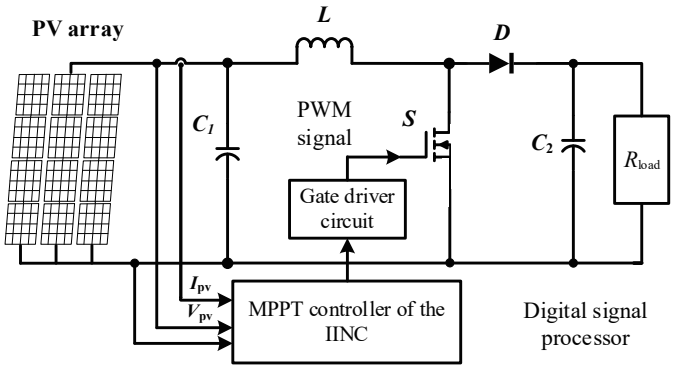

Fig. 3. System architecture of proposed IINC method for MPPT.

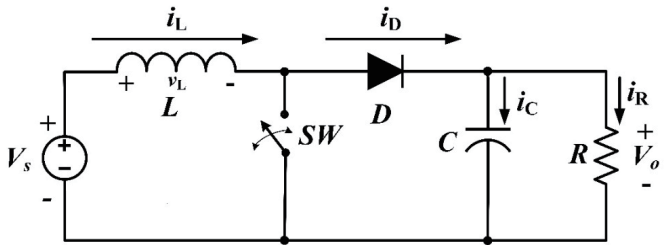

Fig. 4. Boost converter circuit architecture.

Table 3
Component specifications of boost converter.

Component	Specifications
Filter capacitor *C*1	Capacitance 220 µF Voltage rating 400 V
Filter capacitor *C*2	Capacitance 470 µF Voltage rating 500 V
Energy storage inductor *L*	Inductance 1.66 mH Current rating 7.5 A
Fast recovery diode *D* Diode IQBE60E60A1	Voltage rating 600 V Current rating 60 A
Switching transistor - MOSFET IRF460	Voltage rating 500 V Current rating 20 A

used as the basis for determining the MPP. After derivation, Eq. (3) provides the condition for determining the operation at the MPP, where $Gs = -I/V$ represents the static conductance and $G_d = dI/dV$ represents the dynamic conductance. As shown in Fig. 5, if the dynamic conductance dI/dV is greater than the static conductance $-I/V$, the operating point is to the left of the MPP. In this case, the duty cycle (D_k) of the boost converter should be reduced to increase the output voltage of the PVMA. On the other hand, if the dynamic conductance dI/dV is less than the static conductance $-I/V$, the operating point is to the right of the MPP. In this case, the duty cycle (D_k)

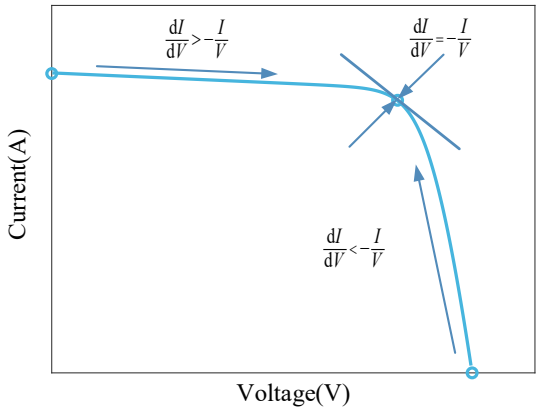

Fig. 5. (Color online) Dynamic and static conductance variations of PVMA.

should be increased to reduce the output voltage of the PVMA until the dynamic conductance dI/dV equals the static conductance $-I/V$, indicating that the MPP has been tracked. The control flow chart for MPPT is shown in Fig. 6. If the tracking step size (perturbation amount) is set smaller, the oscillation around the MPP will be smaller, making it easier to track the true MPP, but the tracking time will increase accordingly. Conversely, if the tracking step size is set larger, the tracking speed will be higher, but it will cause larger oscillations around the MPP, increasing energy loss and reducing the output power of the PVMA.

$$\frac{dP}{dV} = \frac{d(IV)}{dV} = I + \frac{dI}{dV} = 0 \tag{2}$$

$$\frac{dI}{dV} = -\frac{I}{V} \tag{3}$$

4.1 INC method with fixed initial tracking voltage

As shown in the P–V characteristic curve of the PVMA in Fig. 7, the MPP voltage variation under different solar irradiance conditions is minimal. To further improve tracking speed, we propose setting the initial tracking voltage V_{st} to 0.8 times the MPP voltage V_{mp} of the PVMA under standard test conditions (i.e., temperature of 25 °C and irradiance of 1000 W), that is, $V_{st} = 0.8V_{mp}$. This approach shortens the time required to track the MPP and thus improves the power generation efficiency of the photovoltaic system.

4.2 INC method with both fixed initial tracking voltage and adjustable tracking step size

While the INC method with fixed initial tracking voltage can shorten the tracking time, the traditional INC's tracking step size, whether set to be very large or small, can affect the stability and efficiency of the tracking process. To improve the system's steady-state performance, reduce

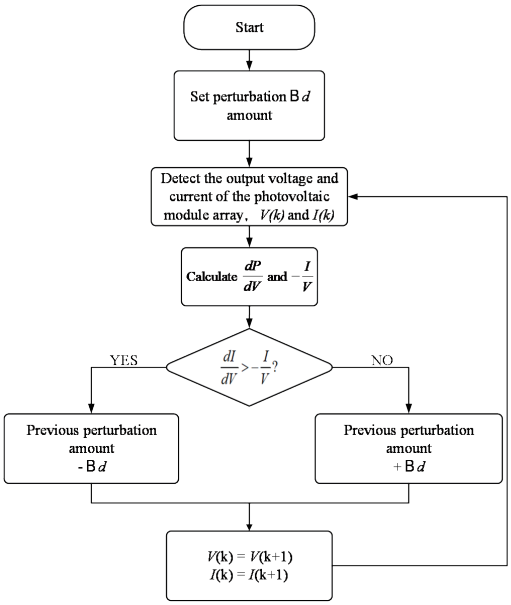

Fig. 6. Control flowchart of traditional INC method.

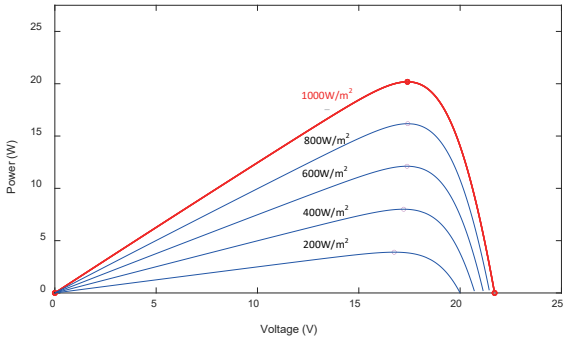

Fig. 7. (Color online) MPP voltage corresponding to different solar irradiance levels in PVMA.

the oscillation amplitude of the tracking, and shorten the MPPT time, we propose not only fixing the initial tracking voltage but also adjusting the duty cycle increment on the basis of the slope change intervals of the *P–V* characteristic curve shown in Table 4. This adjustment automatically reduces the duty cycle variation as the operating point approaches the MPP. As the operating point moves further away from the MPP, the duty cycle variation is increased to enlarge the tracking step size. This enhances the tracking efficiency and reduces the oscillation amplitude as the system approaches the MPP. Additionally, the duty cycle variation can be adjusted in real time to accommodate changes in solar irradiance. Figure 8 shows the slope-region division diagram for the automatic adjustment of the tracking step (i.e., the change in duty cycle) based on the *P–V* characteristic curve as presented in Table 4, using the proposed IINC method. From Fig. 8, it can be observed that when the slope *m* is greater than zero, it indicates that the operating point is to the left of the MPP. In this case, the tracking direction needs to move to the right until the MPP is reached. Conversely, when the slope *m* is less than zero, it indicates that the operating point is on the right side of the MPP, and the tracking direction should move to the left towards the MPP. When the slope *m* equals zero, it indicates that the MPP has been reached. The definition of the slope (*m*) is given in Eq. (4), where P_k and V_k are the current power and voltage values at the operating point, whereas P_{k-1} and V_{k-1} are the power and voltage values at the previous operating point, respectively. Near the MPP, *dP*/*dV* approaches zero, meaning large perturbations would cause oscillation. Therefore, the algorithm applies larger duty cycle increments when |*m*| is large (far from the MPP) and smaller duty cycle increments when |*m*| is small (near MPP), ensuring fast convergence without overshoot.

$$m = \frac{dP}{dV} = \frac{P_k - P_{k-1}}{V_k - V_{k-1}} \tag{4}$$

Table 4
Adjustment relationship for duty cycle variation based on *P–V* characteristic curve slope intervals.

P–V characteristic curve slope interval	Duty cycle variation (Δd)
Interval m_1: $0.5 \leq m \leq 1$	0.008
Interval m_2: $0 < m \leq 0.5$	0.001
Interval m_3: $-0.5 \leq m < 0$	0.002
Interval m_4: $-1 \leq m \leq -0.5$	0.003

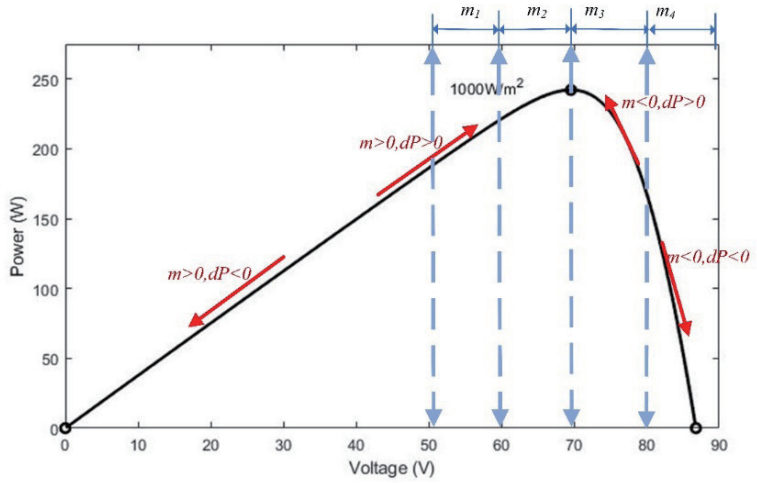

Fig. 8. (Color online) Slope interval classification of duty cycle variation adjustment based on *P–V* characteristic curve in IINC method.

5. Experimental Results

In this study, we used the 62050H-600S programmable DC power supply manufactured by Chroma ATE Inc.[14] to simulate the output characteristics of a four-series, three-parallel PVMA, and performed MPPT using traditional and two improved methods. Figures 9 and 10 show the measured *I–V* and *P–V* characteristic curves of the four-series, three-parallel PVMA at irradiance levels of 1000 and 500 W/m^2, respectively. The hardware circuit for MPPT was completed using Altium Designer software[15] for the wiring and component layout, as shown in Fig. 11. We employed the TMS320F2809 DSP[11] developed by Texas Instruments (USA), which is specifically designed for high-speed numerical computation and control logic, provides higher real-time responsiveness and computational density than conventional microcontrollers, and is therefore highly suitable for application in this study or in more complex MPPT algorithms. Figure 12 shows the test platform setup. The measurement equipment includes a DC power supply, storage oscilloscope, electronic load, programmable DC power supply (PV module array simulator), boost converter, TMS320F2809 DSP, and graphical user interface (GUI) operated via a computer.

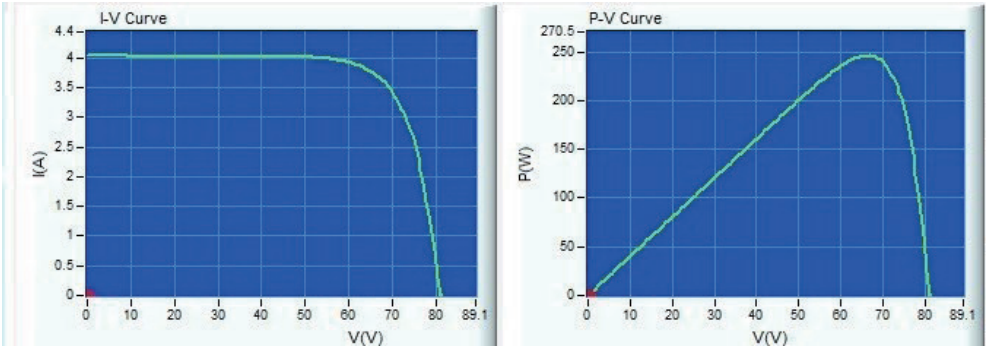

Fig. 9. (Color online) Measured *I–V* and *P–V* output characteristic curves of the four-series, three-parallel PVMA simulator at an irradiance of 1000 W/m^2.

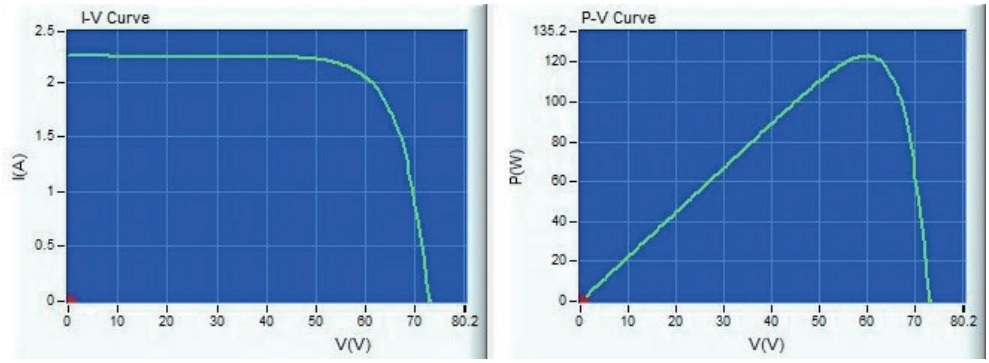

Fig. 10. (Color online) Measured *I–V* and *P–V* output characteristic curves of the four-series, three-parallel PVMA simulator at an irradiance of 500 W/m^2.

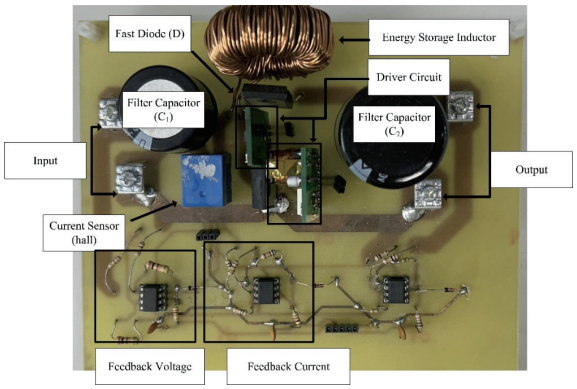

Fig. 11. (Color online) Actual hardware circuit.

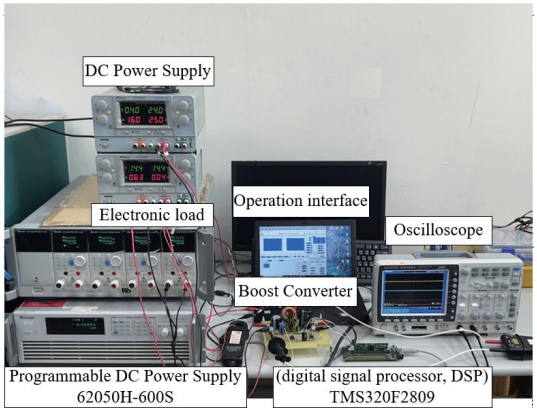

Fig. 12. (Color online) Test platform setup.

Next, MPPT was performed using the traditional INC method and the IINC method. Figures 13 to 15 show the measured results of the PVMA under a solar irradiance of 1000 W/m² and a temperature of 25 °C, utilizing the traditional INC method, the fixed initial tracking voltage

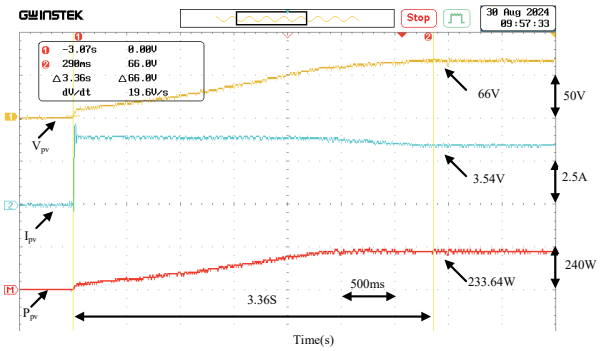

Fig. 13. (Color online) Measured results of MPPT using the traditional INC method under irradiance intensity of 1000 W/m² and temperature of 25°C.

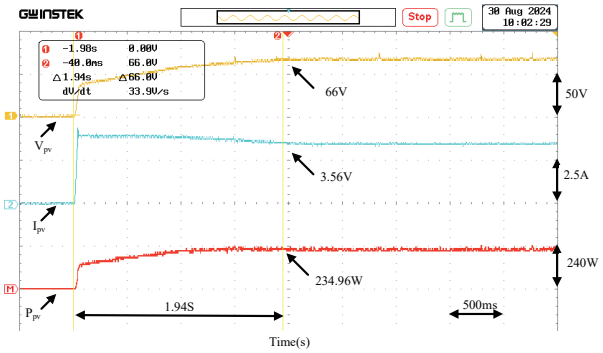

Fig. 14. (Color online) Measured results of MPPT using the INC method with fixed initial tracking voltage under irradiance intensity of 1000 W/m² and temperature of 25°C.

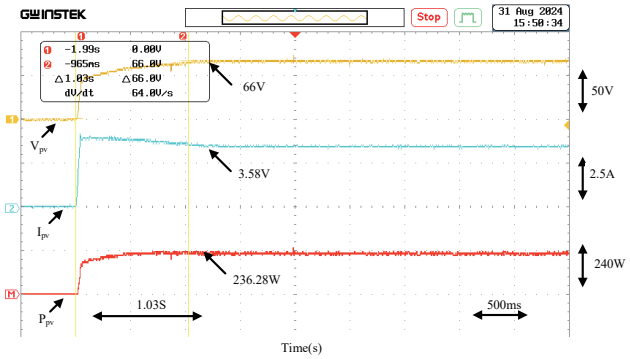

Fig. 15. (Color online) Measured results of MPPT using the INC method with fixed initial tracking voltage and adjustment of tracking step size based on *P–V* characteristic curve slope under irradiance intensity of 1000 W/m² and temperature of 25°C.

method, and the fixed initial tracking voltage method combined with the *P–V* characteristic curve slope adjustment for the INC, respectively. Figures 16 to 18 show the measured results of

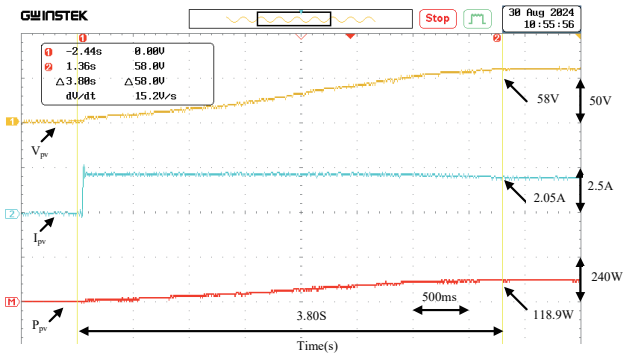

Fig. 16. (Color online) Measured results of MPPT using the traditional INC method under irradiance intensity of 500 W/m² and temperature of 25°C.

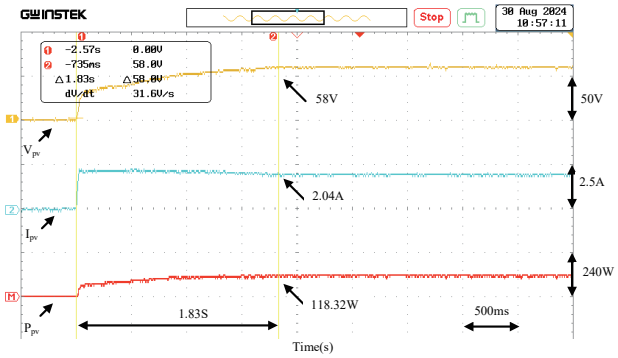

Fig. 17. (Color online) Measured results of MPPT using the fixed initial tracking voltage INC method under irradiance intensity of 500 W/m² and temperature of 25°C.

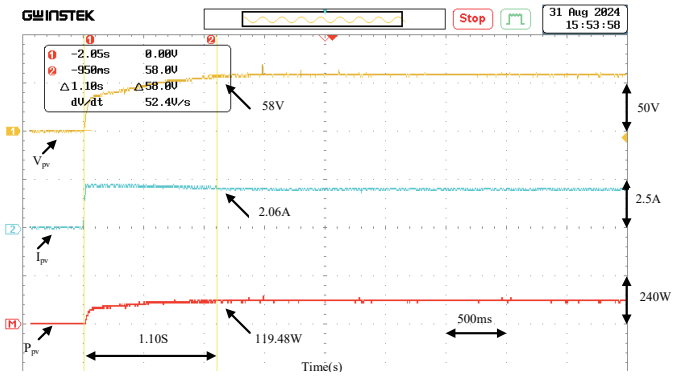

Fig. 18. (Color online) Measured results of MPPT using the fixed initial tracking voltage INC method with *P–V* characteristic curve slope adjustment under irradiance intensity of 500 W/m² and temperature of 25°C.

the PVMA under a solar irradiance of 500 W/m² and a temperature of 25 °C, utilizing the traditional INC method, the fixed initial tracking voltage method, and the fixed initial tracking

voltage method combined with the *P–V* characteristic curve slope adjustment for the INC, respectively.

6. Discussion

From the measured results, it is observed that under an irradiance intensity of 1000 W/m², all three tracking methods successfully tracked the MPP voltage of 66 V, the MPP current of 3.6 A, and the maximum power of 237.6 W. The traditional INC method took 3.36 s to track the MPP, whereas the method using the fixed initial tracking voltage took only 1.94 s. The method combining the fixed initial tracking voltage with the dynamic adjustment of tracking steps based on the *P–V* characteristic curve slope reduced the tracking time further to 1.03 s. In addition, the total harvested energy during a 60 s test increased by approximately 2.8% compared with that obtained by the traditional INC method. Similarly, under an irradiance intensity of 500 W/m², all three tracking methods successfully tracked the MPP voltage of 58 V, the MPP current of 2.05 A, and the maximum power of 118 W. The traditional INC method took 3.80 s to track the MPP, whereas the method using the fixed initial tracking voltage took only 1.83 s. The method combining the fixed initial tracking voltage with the dynamic adjustment of tracking steps based on the *P–V* characteristic curve slope reduced the tracking time further to 1.10 s. The harvested energy gain under this condition was about 2.3% compared with that obtained by the conventional INC method. On the basis of the experimental results, we observed that both IINC methods, under different solar irradiance levels, track the MPP in less time than the traditional INC method. In particular, the method using the fixed initial tracking voltage with the tracking step adjusted on the basis of the *P–V* characteristic curve slope exhibits faster dynamic response. Therefore, the use of the IINC method for MPPT in PVMAs provides higher energy generation efficiency. Therefore, the proposed IINC method not only improves the tracking speed but also enhances the overall energy generation efficiency.

7. Conclusion

In this paper, we proposed an improved version of the traditional INC method for MPPT to enhance the tracking speed and, consequently, improved the output power of the PVMA. First, the initial tracking voltage of the traditional INC method was set to 0.8 times the MPP voltage of the PVMA under standard test conditions. Then, the output *P–V* characteristic curve of the PVMA was divided into four slope regions. On the basis of the region where the operating point was located, the tracking step was automatically adjusted, and this approach was applied to the PVMA for MPPT. In this paper, we presented two IINC methods: one with the fixed initial tracking voltage and the other with the fixed initial tracking voltage combined with the adjustment of the tracking step based on the slope interval of the *P–V* characteristic curve. Among them, the INC method with the fixed initial tracking voltage and the adjustment of the tracking step using the slope interval of the *P–V* characteristic curve showed higher tracking speed and can reduce power losses during tracking, thereby improving overall power generation efficiency. Experimental results demonstrated that when the solar irradiance varies, the proposed IINC methods for MPPT can simultaneously achieve higher dynamic and steady-state response

performance. Future work will focus on integrating MPPT with energy storage systems, applying predictive and AI-based adaptive algorithms, and exploring smart grid connectivity to enhance system efficiency and reliability further.

Acknowledgments

This work was supported by the National Science and Technology Council, Taiwan, under Grant no. NSTC 113-2221-E-167-035-.

References

1 A. Ostadrahimi and Y. Mahmoud: Proc. 2020 Int. Conf. Smart Grids and Energy Systems (IEEE, 2020) 819–825.
2 P. R. S. Preethishri and K. K. Selvi: Proc. 2016 IEEE 1st Int. Conf. Power Electronics, Intelligent Control and Energy Systems (IEEE, 2016) 1–4.
3 A. Al-Subhi and I. El-Amin: Proc. Smart Cities Symp. 2018 (IET, 2018) 1–6.
4 J. Dong, X. Ma, and S. Tuo: Proc. China Int. Conf. Electricity Distribution (IEEE, 2018) 1997–2001.
5 T. T. T. Bau and K. H. Chao: Sens. Mater. **35** (2023) 2637. https://doi.org/10.18494/SAM4353
6 G. Luo, J. Liu, T. Yang, Y. Dou, and N. Chen: Proc. China Int. SAR Symp. (IEEE, 2022) 1–6.
7 W. Libo, Z. Zhengming, and L. Jianzheng: IEEE Trans. Energy Convers. **22** (2007) 881. https://doi.org/10.1109/TEC.2007.895461
8 S. Khadidja, M. Mountassar, and B. M'hamed: Proc. Int. Conf. Green Energy Conversion Systems (IEEE, 2017) 1–6.
9 M. J. Hossain, B. Tiwari, and I. Bhattacharya: Proc. IEEE 43rd Photovoltaic Specialists Conf. (IEEE, 2016) 3230–3233.
10 Kyocera KS20 Solar Panel: https://www.ecodirect.com/Kyocera-KS20-Solar-Panel-20-Watt-12-Volt-p/kyocera-ks20.htm (accessed December 2022).
11 Texas Instruments, TMS320F2809 Datasheet: https://www.ti.com/lit/ds/symlink/tms320f2809.pdf (accessed December 2022).
12 C. Abdelkhalek, E. B. Said, A. Younes, and A. Hassan: Proc. IEEE Int. Conf. Electronics, Control, Optimization and Computer Science (IEEE, 2020) 1–6.
13 D. W. Hart: Introduction to Power Electronics (Pearson Book Company, 2002) 2nd ed., pp. 221–237.
14 Chroma ATE Inc., 62000H Series DC Power Supply: https://www.chromaate.com/en/product/dc_power_supply_62000h_series_203 (accessed December 2022).
15 J. Wang and T. T. Liu: Proc. Chinese Control Decision Conf. (IEEE, 2018) 3457–3460.

About the Authors

Kuei-Hsiang Chao received his B.S. degree in electrical engineering from National Taiwan University of Science and Technology, Taipei, Taiwan, in 1988, and his M.S. and Ph.D. degrees in electrical engineering from National Tsing Hua University, Hsinchu, Taiwan, in 1990 and 2000, respectively. He is presently a tenured distinguished professor at National Chin-Yi University of Technology, Taichung, Taiwan. His areas of interest are computer-based control systems, applications of control theory, renewable energy, and power electronics. Dr. Chao is a life member of the Solar Energy and New Energy Association and a member of the IEEE. He is also a Fellow of the Taiwan Power Electronics Association (TaiPEA) and Taiwan Association for Academic Innovation (TAAI).

Cheng-Ze Li was born in Taipei, Taiwan, in 2003. He is currently studying in the Department of Electrical Engineering at National Chin-Yi University of Technology. His areas of interest are computing applications, power electronics, and maximum power point tracking for photovoltaic module arrays.

Kuan-Ting Lee was born in Taipei, Taiwan, in 2003. He is currently a senior undergraduate student in the Department of Electrical Engineering at National Chin-Yi University of Technology, Taichung, Taiwan. His areas of interest include energy technology, power electronics, and maximum power point tracking for photovoltaic module arrays.